simula

waterscales

European Research Council
Established by the European Commission

The Research Council of Norway

Compatible discretizations in our hearts and minds

Marie E. Rognes

ENUMATH, Voss, Norway

Sept 28 2017

Act I: Simulating the brain's waterscape

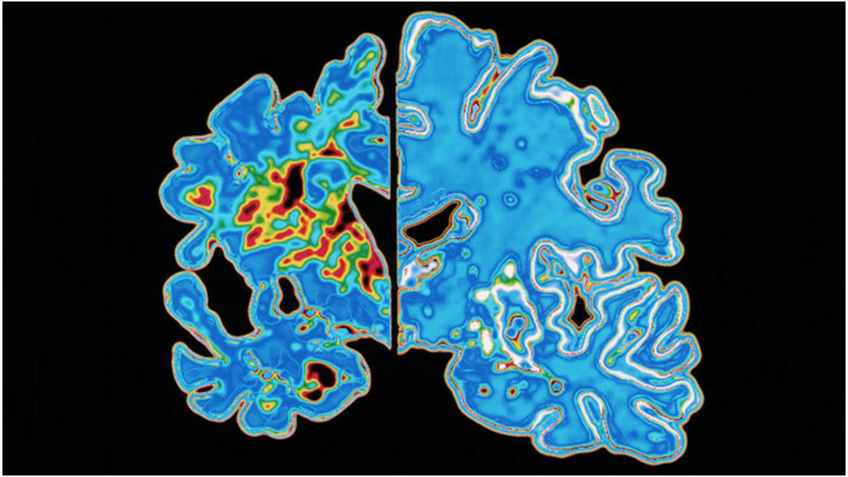

The brain of a person with Alzheimer's (left) is shrunken, compared with a normal brain (right), from nerve cell death, and a new drug has failed to stem such neurodegeneration. Alfred Pasieka/Science Source

Another Alzheimer's drug flops in pivotal clinical trial

By **John Carroll, Endpoints News** | Feb. 15, 2017 , 11:00 AM

Several neurodegenerative diseases are associated with abnormal aggregations of proteins in the brain nerve cells

Alzheimer's disease: extracellular aggregations of β-amyloid in the gray matter of the brain

[Glenner and Wong, Biochem Biophys ..., 1984; Selkoe, Neuron, 1991]

Parkinson's disease/Dementia with Lewy bodies: aggregations of α-synuclein in neurons

[Dawson and Dawson, Science, 2003; McKeith et al, Lancet, 2004]

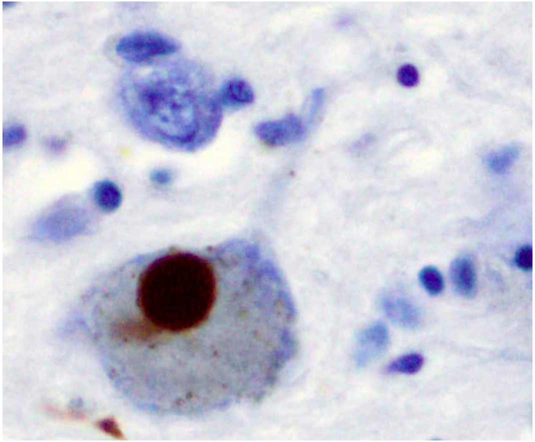

Lewy-body (brown) in Parkinson's disease

[Wikimedia Commons]

The lymphatic system clears the body of metabolic waste, what plays the role of the lymphatics in the brain?

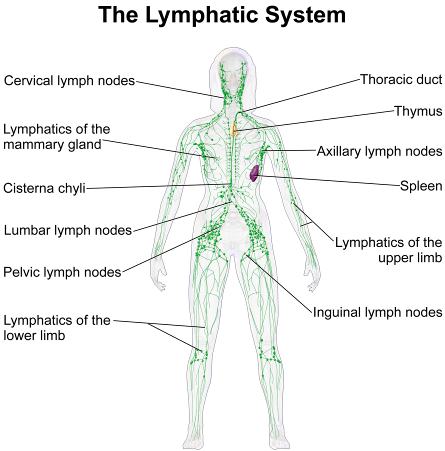

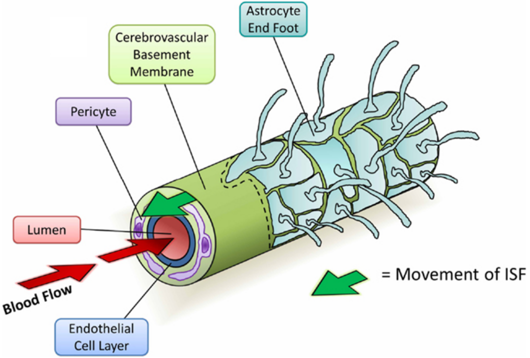

[Wikimedia Commons, Morris et al [2014]]

In the context of cerebral fluid flow and transport, the brain can be viewed as a multi-porous and elastic medium

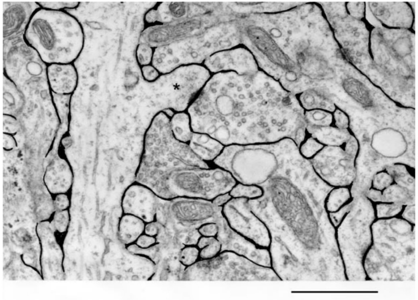

A small region of rat cerebral cortex with black areas representing extracellular space (Scale bar: $\approx 1\mu$m)

[Nicolson, 2001]

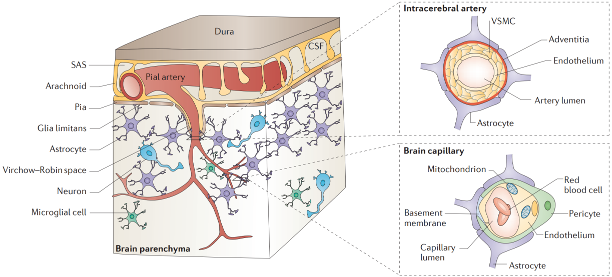

The brain parenchyma includes multiple fluid networks (extracellular spaces, arteries, capillaries, veins, paravascular spaces)

[Zlokovic, 2011]

Multiple-network poroelastic theory (MPET) is a macroscopic model for poroelastic media with multiple fluid networks

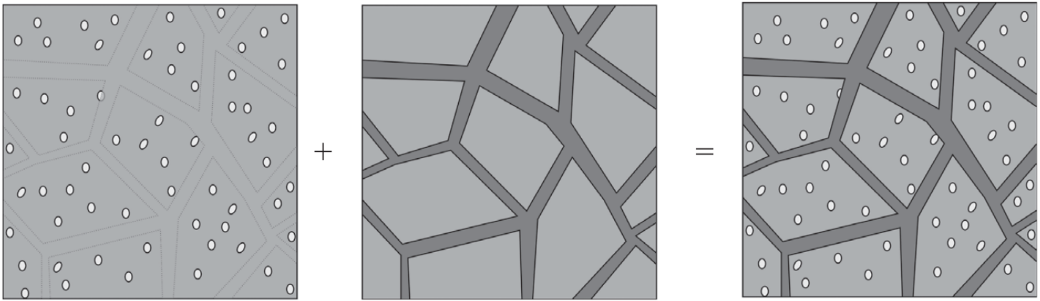

[Bai, Elsworth, Roegiers (1993); Tully and Ventikos (2011)]

The MPET equations describe displacement and A-network pressures under balance of momentum and mass

Given $A \in \mathbb{N}$, f and g_a, find the displacement $u(x,t)$ and the pressures $p_a = p_a(x,t)$ for $a = 1, \ldots, A$ such that

$$\rho \ddot{u} - \operatorname{div}(\sigma^* - \textstyle\sum_a \alpha_a p_a \, \mathrm{I}) = f,$$
$$- \operatorname{div} \rho_a K_a \ddot{u} + c_a \dot{p}_a + \alpha_a \operatorname{div} \dot{u} - \operatorname{div} K_a \operatorname{grad} p_a + S_a = g_a, \quad a = 1, \ldots, A,$$

Transfer between networks:

$$S_a = \textstyle\sum_b s_{a \leftarrow b} = \sum_b \xi_{a \leftarrow b} (p_a - p_b),$$

Linearly elastic (isotropic) tissue matrix/pseudo-stress:

$$\sigma^*(u) = 2\mu \varepsilon(u) + \lambda \operatorname{div} u \, \mathrm{I},$$

$A = 1$ corresponds to Biot's equations, $A = 2$ Barenblatt-Biot. $\lambda \to \infty$, $c_a \to 0$ and $K \to 0$ interesting regimes.

Standard finite element formulation suffers from Poisson locking (loss of convergence) in the incompressible limit $\lambda \to \infty$

	$\|u - u_h\|_{L^\infty(0,T,L^2)}$	Rate	$\|u - u_h\|_{L^\infty(0,T,H^1)}$	Rate
h	0.169		2.066	
$h/2$	0.040	2.09	0.980	1.08
$h/4$	0.010	2.04	0.480	1.03
$h/8$	0.002	2.03	0.235	1.03
$h/16$	0.001	2.09	0.110	1.10
Optimal		3		2

Test case A: Smooth manufactured solution test case inspired by [Yi, 2017 [Section 7.1]] with $\operatorname{div} u \to 0$ as $\lambda \to \infty$, but linear in time, $A = 2$, $T = 0.5$, $\mu = 0.33$, $\lambda = 1.67 \times 10^4$, $S = 0$, all other parameters 1, Crank-Nicolson discretization in time. Standard Taylor-Hood $(u_h, p_h) \in \mathcal{P}_2^d \times \mathcal{P}_1^A$ discretization in space:

$$
\begin{aligned}
(\sigma^*(u), \operatorname{grad} v) - \textstyle\sum_a (\alpha_a p_a, \operatorname{div} v) &= (f, v) \qquad \forall\, v \in V_h \\
(c_a \dot{p}_a + \alpha_a \operatorname{div} \dot{u} + S_a, q_a) + (K_a \operatorname{grad} p_a, \operatorname{grad} q_a) &= (g_a, q_a) \quad \forall\, q_a \in Q_{a,h}
\end{aligned}
$$

Extensive research on robust finite element methods for Biot's equations for all relevant parameter regimes

- Stokes-type (two-field) formulations for solid displacement and pore pressure: $(u, p) \in H^1(\Omega; \mathbb{R}^d) \times H^1(\Omega)$;

  [Murad, Thomée and Loula (1992-1996)]

- Elasticity/Darcy-type (three-field) formulations for solid displacement, fluid velocity and pore pressure: $(u, v, p) \in H^1(\Omega; \mathbb{R}^d) \times H(\mathrm{div}, \Omega) \times L^2(\Omega)$;

  [Phillips and Wheeler (2007-2008)]

- Mixed Elasticity/Darcy-type (four-field) formulations for solid displacement, pseudo-stress tensor, fluid flux, pore pressure: (u, σ^*, v, p);

  [Korsake and Starke (2005), Yi (2014), Lee (2016)]

- Stabilization techniques;

  [Aguilar, Gaspar, Lisbona, and Rodrigo (2008); many others]

- Total pressure formulation;

  [Ruiz-Bayer (2016); Lee, Mardal and Winther (2017)]

Preliminaries and notation for total-pressure augmented variational formulation of the quasi-static MPET equations

Let $\Omega \subset \mathbb{R}^d$ with boundary $\partial\Omega$ and $T > 0$. Minimal complexity boundary conditions:

$$\begin{aligned} u &= 0 \quad \text{on } \Gamma \subset \partial\Omega \\ \sigma \cdot n \equiv (\sigma^*(u) - \textstyle\sum_a \alpha_a \operatorname{grad} p_a) \cdot n &= 0 \quad \text{on } \partial\Omega - \Gamma \neq \emptyset \\ p_a &= 0 \quad \text{on } \partial\Omega, \quad a = 1, \ldots, A \end{aligned}$$

Initial conditions for the displacement and all pressures:

$$u(t = 0) = u_0, \quad p_a(t = 0) = p_{a,0} \quad a = 1, \ldots, A$$

Define $V = \{v \in H^1(\Omega; \mathbb{R}^d) \text{ s.t. } v|_\Gamma = 0\}$, $Q_0 = L^2(\Omega)$, $Q_a = H_0^1(\Omega)$, $a = 1, \ldots, A$.

$$(a, b) \equiv \int_\Omega a \cdot b \, \mathrm{d}x, \quad (a, b)_\beta \equiv \int_\Omega \beta a \cdot b \, \mathrm{d}x, \quad \|a\|_\beta^2 \equiv (a, a)_\beta \quad \beta \in \mathbb{R}^+$$

Introducing a total-pressure-augmented variational formulation of the MPET equations

Key idea: inspired by [Lee, Mardal, Winther, 2017]: introduce the total pressure

$$p_0 = \lambda \operatorname{div} u - \sum_{a=1}^{A} \alpha_a p_a \leftrightarrow \operatorname{div} u = \lambda^{-1} \alpha \cdot p$$

with $\alpha = (1, \alpha_1, \ldots, \alpha_A)$, $p = (p_0, \ldots, p_A)$.

Variational formulation of total-pressure augmented quasi-static MPET

Given g_a for $a = 1, \ldots, A$, find $u \in H^1((0,T]; V)$ and $p_a \in H^1((0,T]; Q_a)$ for $a = 0, \ldots, A$ such that

$$\begin{aligned}
(2\mu\varepsilon(u), \varepsilon(v)) + (p_0, \operatorname{div} v) &= 0 && \forall\, v \in V \\
(\operatorname{div} u, q_0) - (\lambda^{-1}\alpha \cdot p, q_0) &= 0 && \forall\, q_0 \in Q_0 \\
(c_a \dot{p}_a + \alpha_a \lambda^{-1} \alpha \cdot \dot{p} + S_a, q_a) + (K_a \operatorname{grad} p_a, \operatorname{grad} q_a) &= (g_a, q_a) && \forall\, q_a \in Q_a, a = 1, \ldots, A
\end{aligned}$$

[Lee, Mardal, Piersanti, R., in prep., 2017]

In the incompressible limit $\lambda \to \infty$, the total-pressure augmented quasi-static MPET system decouples

In the incompressible limit $\lambda \to \infty$, the total-pressure augmented quasi-static MPET system decouple to an incompressible Stokes system and a set of parabolic/elliptic equations.

Find $u \in H^1((0,T];V)$ and $p_a \in H^1((0,T];Q_a)$ for $a = 0, \ldots, A$ such that

$$
\begin{aligned}
(2\mu\varepsilon(u), \varepsilon(v)) + (p_0, \operatorname{div} v) &= 0 && \forall\, v \in V \\
(\operatorname{div} u, q_0) &= 0 && \forall\, q_0 \in Q_0 \\
(c_a \dot{p}_a + S_a, q_a) + (K_a \operatorname{grad} p_a, \operatorname{grad} q_a) &= (g_a, q_a) && \forall\, q_a \in Q_a
\end{aligned}
$$

Robust energy estimate for total-pressure augmented quasi-static MPET

Theorem

Assume that $u \in H^1((0,T];V)$ and $p_a \in H^1((0,T];Q_a)$ are solutions of the total-pressure augmented quasi-static MPET variational formulation. Then for all $t \in (0,T]$ and uniformly in λ, c_a:

$$\|\varepsilon(u(t))\|_{2\mu} + \sum_{a=1}^{A} \|p_a(t)\|_{c_a} + \|\alpha \cdot p(t)\|_{\lambda^{-1}} + \sum_{a=1}^{A} \| \|\operatorname{grad} p_a\|_{K_a} \|_{L^2(0,t)}$$
$$\lesssim \|\varepsilon(u(0))\|_{2\mu} + \sum_{a=1}^{A} \|p_a(0)\|_{c_a} + \|\alpha \cdot p(0)\|_{\lambda^{-1}} + \sum_{a=1}^{A} \| \|g_a\| \|_{L^2(0,t)}$$

Proof.

Standard techniques, summing with $v = \dot{u}$, $q_a = p_a$ for $a = 1, \dots, A$, $q_0 = -p_0$ in time-derivative of 2nd eq., combined with improved Grönwall-type estimate. $\square$

Introducing compatible discrete finite element spaces

Let $\mathcal{T}_h$ denote a conforming, shape-regular, simplicial discretization of Ω with discretization size $h > 0$. Relative to $\mathcal{T}_h$, we define finite element spaces $V_h \subset V$ and $Q_{a,h} \subset Q_a$ for $a = 0, \dots, A$.

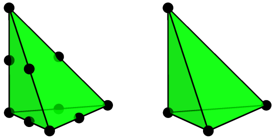

Assume that

A1: $V_h \times Q_{0,h}$ is a stable (in the Brezzi sense) finite element pair for the Stokes equations;

A2: $Q_{a,h}$ is Poisson-convergent finite element of polynomial order l_a for $a = 1, \dots, A$.

These two assumptions are fulfilled by for instance:

- $V_h \times Q_h = \mathcal{P}_{l+1}(\mathcal{T}_h) \times \mathcal{P}_l^{A+1}(\mathcal{T}_h)$ for $l = 1, \dots,$ (Taylor-Hood-type elements).

Semi-discrete variational formulation of the total-pressure augmented quasi-static MPET equations

Semi-discrete variational formulation of total-pressure quasi-static MPET

For $t \in (0, T]$, find $u_h(t) \in V_h$ and $p_{a,h}(t) \in Q_{a,h}$ for $a = 0, \dots, A$ such that

$$\begin{aligned}
(2\mu\varepsilon(u_h), \varepsilon(v)) + (p_{0,h}, \operatorname{div} v) &= 0 & \forall\, v \in V_h,\\
(\operatorname{div} u_h, q_0) - (\lambda^{-1}\alpha \cdot p_h, q_0) &= 0 & \forall\, q_0 \in Q_{0,h},\\
(c_a \dot{p}_{a,h} + \alpha_a \lambda^{-1} \alpha \cdot \dot{p}_h + S_{a,h}, q_a) + (K_a \operatorname{grad} p_{a,h}, \operatorname{grad} q_a) &= (g_a, q_a) & \forall\, q_a \in Q_{a,h},
\end{aligned}$$

for $a = 1, \dots, A$. Here $S_{a,h} = \sum_{i=1}^{A} \xi_{a \leftarrow b}(p_{a,h} - p_{b,h})$ and $p_h = (p_{0,h}, \dots, p_{A,h})$.

Introducing Stokes-type and weighted elliptic-type projections as auxiliary interpolation operators

For any $(u, p_0) \in V \times Q_0$, define the interpolant $(\Pi_h^V u, \Pi_h^{Q_0} p_0) \in V_h \times Q_{0,h}$ as the unique (**A1**) solution of:

$$
\begin{aligned}
(2\mu\varepsilon(\Pi_h^V u), \varepsilon(v)) + (\Pi_h^{Q_0} p_0, \operatorname{div} v) &= (2\mu\varepsilon(u), \varepsilon(v)) + (p_0, \operatorname{div} v) \quad && \forall\, v \in V_h, \\
(\operatorname{div} \Pi_h^V u, q_0) &= (\operatorname{div} u, q_0) && \forall\, q_0 \in Q_{0,h}.
\end{aligned}
$$

For any $p_a \in Q_a$, define the interpolant $\Pi_h^{Q_a} p_a \in Q_{a,h}$ as the unique (**A2**) solution of:

$$
(K_a \operatorname{grad} \Pi_h^{Q_a} p_a, q_a) = (K_a \operatorname{grad} p_a, \operatorname{grad} q_a) \quad \forall\, q_a \in Q_{a,h}.
$$

For example, for Taylor-Hood type elements of order l:

$$
\begin{aligned}
\|u - \Pi_h^V u\|_1 + \|p_0 - \Pi_h^{Q_0} p_0\|_0 &\lesssim h^m \left(\|u\|_{m+1} + \|p_0\|_m\right) \quad && 1 \le m \le l+1, \\
\|p_a - \Pi_h^{Q_a} p_a\|_0 \lesssim h \|p_a - \Pi_h^{Q_a} p_a\|_1 &\lesssim h^{m+1} \|p_a\|_{m+1} && 1 \le m \le l.
\end{aligned}
$$

Uniform semi-discrete a-priori discretization error estimates for the quasi-static total pressure augmented MPET equations

Introduce standard error decomposition

$$
\begin{aligned}
e_u &\equiv e_u^I + e_u^h, \quad e_u^I \equiv u - \Pi_h^V u, \quad e_u^h \equiv \Pi_h^V u - u_h; \\
e_{p_a} &\equiv e_{p_a}^I + e_{p_a}^h, \quad e_{p_a}^I \equiv p_a - \Pi_h^{Q_a} p_a, \quad e_{p_a}^h \equiv \Pi_h^{Q_a} p_a - p_{a,h} \quad a = 0, \dots, A.
\end{aligned}
$$

Lemma

The discretization errors of the total pressure augmented, quasi-static MPET equations, with Taylor-Hood-type elements of order l, are bounded uniformly in h, c_a and λ:

$$
\begin{aligned}
&\|\varepsilon(e_u^h(t))\|_{2\mu} + \textstyle\sum_{a=1}^A \|e_{p_a}^h(t)\|_{c_a} + \|\alpha \cdot e_p^h(t)\|_{\lambda^{-1}} + \textstyle\sum_{a=1}^A \| \| \operatorname{grad} e_{p_a}^h \|_{K_a} \|_{L^2(0,t)} \\
&\lesssim h^{m+1} \left(E(0)_{\mu, c_a, \lambda^{-1}} + \| \|p\|_{m+1,\lambda^{-1}} \|_{L^1(0,t)} + \textstyle\sum_{a=1}^A \|c_a \|\dot{p}_a\|_{m+1} + \|p\|_{m+1} \|_{L^2(0,t)} \right)
\end{aligned}
$$

for $1 \leq m \leq l$.

Proof.

As for energy estimate using auxiliary interpolation estimates. $\square$

The total-pressure augmented formulation restores optimal convergence, including in the incompressible limit

	$\|u - u_h\|_{L^\infty(0,T,L^2)}$	Rate	$\|u - u_h\|_{L^\infty(0,T,H^1)}$	Rate
h	6.27×10^{-2}		1.46×10^{0}	
$h/2$	7.28×10^{-3}	3.11	3.95×10^{-1}	1.88
$h/4$	8.70×10^{-4}	3.06	1.01×10^{-1}	1.97
$h/8$	1.07×10^{-4}	3.02	2.55×10^{-2}	1.99
$h/16$	1.33×10^{-5}	3.01	6.38×10^{-3}	2.00
Optimal		3		2

	$\|p_1 - p_{1,h}\|_{L^\infty(0,T,L^2)}$	Rate	$\|p_1 - p_{1,h}\|_{L^\infty(0,T,H^1)}$	Rate
h	1.53×10^{-1}		1.68×10^{0}	
$h/2$	4.07×10^{-2}	1.91	8.65×10^{-1}	0.96
$h/4$	1.03×10^{-2}	1.98	4.35×10^{-1}	0.99
$h/8$	2.60×10^{-3}	1.99	2.18×10^{-1}	1.00
$h/16$	6.49×10^{-4}	2.00	1.09×10^{-1}	1.00
Optimal		2		1

Test case A with total-pressure augmented Taylor-Hood $\mathcal{P}_2^d \times \mathcal{P}_1^{A+1}$ discretization.

The total-pressure augmented formulation restores optimal convergence, including in the incompressible limit and zero saturation coefficient

	$\|u - u_h\|_{L^\infty(0,T,L^2)}$	Rate	$\|u - u_h\|_{L^\infty(0,T,H^1)}$	Rate
h	6.27×10^{-2}		1.46×10^{0}	
$h/2$	7.28×10^{-3}	3.11	3.95×10^{-1}	1.88
$h/4$	8.70×10^{-4}	3.06	1.01×10^{-1}	1.97
$h/8$	1.07×10^{-4}	3.02	2.55×10^{-2}	1.99
$h/16$	1.33×10^{-5}	3.01	6.38×10^{-3}	2.00
Optimal		3		2

	$\|p_1 - p_{1,h}\|_{L^\infty(0,T,L^2)}$	Rate	$\|p_1 - p_{1,h}\|_{L^\infty(0,T,H^1)}$	Rate
h	1.58×10^{-1}		1.68×10^{0}	
$h/2$	4.22×10^{-2}	1.90	8.65×10^{-1}	0.96
$h/4$	1.08×10^{-2}	1.97	4.35×10^{-1}	0.99
$h/8$	2.70×10^{-3}	1.99	2.18×10^{-1}	1.00
$h/16$	6.76×10^{-4}	2.00	1.09×10^{-1}	1.00
Optimal		2		1

Test case A with total-pressure augmented Taylor-Hood $\mathcal{P}_2^d \times \mathcal{P}_1^{A+1}$ discretization but with $c_a = 0$.

Total-pressure augmented variational formulation yields natural robust block-diagonal preconditioner

Total-pressure MPET operator (time-discrete)

$$\mathcal{A}_{\Delta t} : H_0^1 \times L_2 \times (H_0^1)^A \to H^{-1} \times L_2 \times (H^{-1})^A$$

Block-diagonal preconditioner

$$P^{-1} A_{\Delta t} x_{\Delta t} \approx P^{-1} b_{\Delta t}$$

$$\mathcal{P} = \operatorname{diag} \begin{pmatrix} -\mu \operatorname{div} \operatorname{grad} \\ I \\ (c_a + \alpha_a \lambda^{-1}) I + \Delta t \, S_a - \Delta t K_a \operatorname{div} \operatorname{grad} \end{pmatrix}$$

[Piersanti, Lee, R., Mardal, in prep., 2017]

		N			
λ	$K_{1,2}$	8	16	32	64
10^0	10^0	56	57	56	55
	10^{-3}	60	61	65	68
	10^{-5}	60	61	65	65
	10^{-8}	61	61	64	65
10^3	10^0	68	72	73	73
	10^{-3}	70	72	73	73
	10^{-5}	71	73	72	73
	10^{-8}	71	72	72	53
10^5	10^0	78	52	53	54
	10^{-3}	52	54	50	54
	10^{-5}	53	54	54	55
	10^{-8}	54	52	52	55

iterations for linear solver convergence (FEniCS, PETSc, Minres, AMG (hypre))

Investigating paravascular fluid flow driven by subarachnoid space arterial pressure variations in the murine brain

Pressure pulsation on outer boundary: $\sigma \cdot n = p_{\mathrm{sas}} \cdot n$ with $p_{\mathrm{sas}} = 0.008 \times 133 \sin(2\pi t)$ (Pa)

Semi-permeable outer and inner membranes: $-K \operatorname{grad} p \cdot n = \beta(p - p_{\mathrm{in}})$.

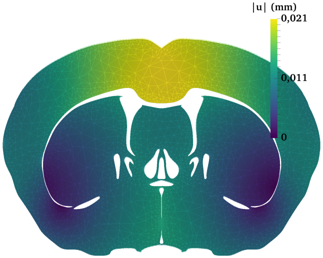

Displacement

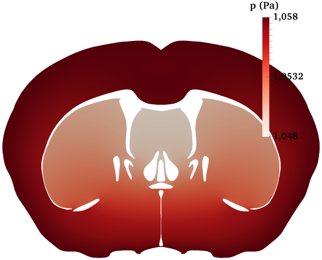

Paravascular fluid pressure

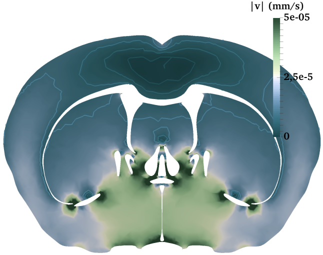

Paravascular fluid velocity

[Simulations courtesy of M. Croci; Mesh courtesy of Allen Brain Atlas, Alexandra Diem and Janis Grobovs]

[Vinje, Croci, Mardal, R., in prep., 2017]

How will a highly uncertain permeability field affect peak paravascular flow?

(u, p) quasi-static MPET solutions, $v = -K\phi^{-1} \operatorname{grad} p$.

Assume that K is a stochastic field:

$$
\begin{aligned}
K(x, (\alpha, \beta)) &= K_0 e^{u(x,\alpha)} 10^{v(\beta)}, \quad x \in \Omega \\
u(x, \cdot) &\sim \mathcal{N}(\mu, \sigma^2) \,|\, \mathbb{E}[e^{u(x,\cdot)}] = 1, \mathbb{V}[e^{u(x,\cdot)}]^{1/2} = 0.2 \\
v(\cdot) &\sim \mathcal{U}(-2, 2),
\end{aligned}
$$

Output functional: $\mathcal{F}(\alpha, \beta) = C \max_{t \in (0,T]} \int_{\mathrm{ROI}} |v(t)| \, \mathrm{d}x \, (\alpha, \beta)$

Preliminary estimates: $P(\mathcal{F} \in [0, 8 \times 10^{-5}] \, \mathrm{mm/s}) \approx 0.95$

$$
\begin{aligned}
\mathbb{E}[\mathcal{F}] &\approx 2.5 \times 10^{-5} \text{mm/s} \\
\mathbb{V}[\mathcal{F}] &\approx (3.2 \times 10^{-5} \text{mm/s})^2
\end{aligned}
$$

Techniques: MLMC, white noise on non-nested mesh hierarchies.

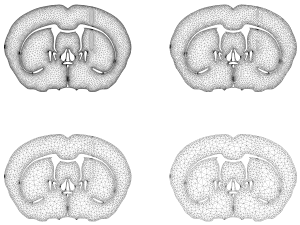

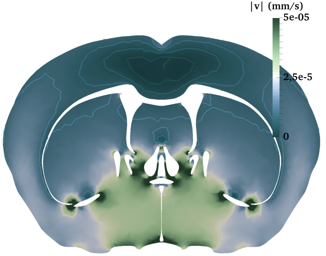

[Croci, R., Farrell, Giles, in prep., 2017]

Act II: Finite collections of biological cells

The paradigm in computational cardiac modelling has been classical homogenized models (bidomain, monodomain)

$$
\begin{aligned}
v_t - \operatorname{div}(M_i \operatorname{grad} v + M_i \operatorname{grad} u_e) &= -I_{\text{ion}}(v, s) \\
\operatorname{div}(M_i \operatorname{grad} v + (M_i + M_e) \operatorname{grad} u_e) &= 0 \\
s_t &= F(v, s)
\end{aligned}
$$

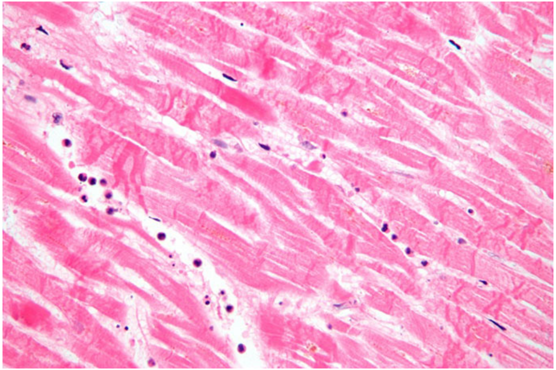

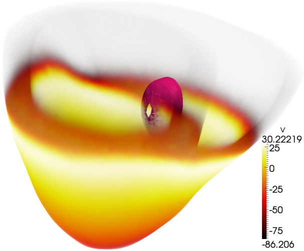

Heart cell: $h \approx 100\mu$m
FEM cell: $h \leq 100\mu$m (!)

Heart cells beating in a Petri dish offer new hope to heart patients

Ingenious use of stem cell research brings treatment for incurable condition closer

Stem cells in a laboratory: the red areas are cells beginning to specialise as heart muscle. Photograph: Medica Research Council

[The Guardian, Feb 2 2014]

The emerging EMI framework use a geometrically explicit representation of the cellular domains

Find the intracellular potential u_i in $\Omega_i = \cup_k \Omega_i^k \subset \mathbb{R}^d$, the extracellular potential u_e in $\Omega_e \subset \mathbb{R}^d$ and the membrane potential v (and other membrane variables) on $\Gamma = \Gamma_1 \cup \Gamma_2 \cup \Gamma_{1,2}$.

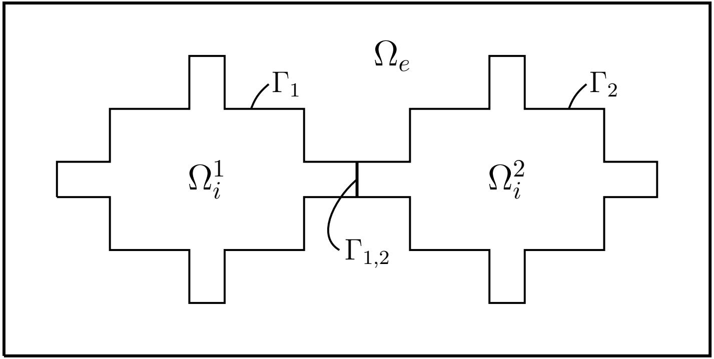

[Stinstra et al, 2010; Agudelo-Toro and Neef, 2013]

The EMI equations describe the dynamics of extracellular, membrane and intracellular electrical potentials

Find the electric potential $u(t) : \Omega \to \mathbb{R}$, and the transmembrane potential $v(t) : \Gamma \to \mathbb{R}$ s.t:

$$
\begin{aligned}
\operatorname{div} \sigma \operatorname{grad} u &= f \quad \text{in } \Omega_i, \Omega_e \\
C_m v_t + \sigma \operatorname{grad} u \cdot n|_{\Omega_i} + I_{\text{ion}}(v) &= 0 \quad \text{on } \Gamma,
\end{aligned}
$$

with interface conditions on Γ

$$
\begin{aligned}
[\![u]\!] &= v, \quad \text{(v is the jump in u)} \\
[\![\sigma \operatorname{grad} u \cdot n]\!] &= 0 \quad \text{(continuity of flux/current)}
\end{aligned}
$$

Boundary condition $u = 0$ on $\partial\Omega$ and initial conditions for v.

For now, $I_{\text{ion}}(v) = v$. (Generally $I_{\text{ion}} = I(v, s)$ highly non-linear.)

[Stinstra et al, 2010; Agudelo-Toro and Neef, 2013]

Introducing an H(div)-based variational formulation for the EMI equations

Introduce $s = \sigma \operatorname{grad} u$ in Ω_i and Ω_e.

Let

$$U = L^2(\Omega), \quad S = H(\operatorname{div}, \Omega), \quad V = H^{\frac{1}{2}}(\Gamma)$$

Note that $\operatorname{tr}_\Gamma S = H^{-1/2}(\Gamma)$.

Variational formulation

Find $u(t) \in U$, $s(t) \in S$ and $v(t) \in V$ satisfying

$$\begin{aligned}
(\operatorname{div} s, \phi) &= (f, \phi) & \forall\, \phi \in U, \\
(\sigma^{-1} s, \tau) + (\operatorname{div} \tau, u) - \langle \tau \cdot n, v \rangle_\Gamma &= 0 & \forall\, \tau \in S, \\
-(C_m v_t + I_{\text{ion}}(v), w)_\Gamma - \langle s \cdot n, w \rangle_\Gamma &= 0 & \forall\, w \in V.
\end{aligned}$$

where n is an outward normal on Γ and $(\cdot, \cdot)$ is the $L^2(\Omega)$-norm and $\langle \cdot, \cdot \rangle_\Gamma$ the duality pairing on $H^{-1/2}(\Gamma) \times H^{1/2}(\Gamma)$.

[Tveito, Jæger, Kuchta, Mardal, R., 2017]

Semi-discrete H(div)-conforming mixed finite element formulation for the EMI equations

Take a mesh $\mathcal{T}_h$ of Ω that conforms to Ω_i, Ω_e and Γ, and denote by Γ_h the resulting mesh of Γ. Define $S_h \subseteq S$, $U_h \subseteq U$ and $V_h \subseteq V$ for instance:

$$S_h = RT_j(\mathcal{T}_h), \quad U_h = \mathcal{P}_{j-1}(\mathcal{T}_h), \quad V_h = \mathcal{P}_{j-1}(\Gamma_h)$$

for $j = 1, 2, \ldots$ where $\mathcal{P}$ denotes the space of (discontinuous) piecewise polynomials defined relative to the relevant mesh.

Semi-discrete finite element formulation

Find $u_h \in U_h$, $s \in S_h$ and $v \in V_h$ satisfying

$$\begin{aligned}
(\operatorname{div} s_h, \phi) &= 0 \quad \forall\, \phi \in U_h, \\
(\sigma^{-1} s_h, \tau) + (\operatorname{div} \tau, u_h) - \langle \tau \cdot n, v_h \rangle_\Gamma &= 0 \quad \forall\, \tau \in S_h, \\
-(C_m v_{h,t} + I_{\text{ion}}(v_h), w)_\Gamma - \langle s_h \cdot n, w \rangle_\Gamma &= 0 \quad \forall\, w \in V_h.
\end{aligned}$$

[Tveito, Jæger, Kuchta, Mardal, R., 2017]

H(div)-based formulation converges at optimal rates for the EMI equations

n	$\|u-u_h\|_0$	$\|\hat{J}-\hat{J}_h\|_0$	$\|\hat{J}-\hat{J}_h\|_{\mathrm{div}}$	$\|v-v_h\|_0$	$\|u-u_h\|_\infty$	$\|v-v_h\|_\infty$
16	8.41E-02(--)	6.49E-01(--)	6.62E+00(--)	1.02E-01(--)	2.73E-02(--)	2.53E-03(--)
32	4.21E-02(1.00)	3.24E-01(1.00)	3.32E+00(0.99)	5.13E-02(1.00)	6.87E-03(1.99)	6.36E-04(1.99)
64	2.11E-02(1.00)	1.62E-01(1.00)	1.66E+00(1.00)	2.56E-02(1.00)	1.72E-03(2.00)	1.57E-04(2.02)
128	1.05E-02(1.00)	8.10E-02(1.00)	8.31E-01(1.00)	1.28E-02(1.00)	4.30E-04(2.00)	3.76E-05(2.06)
256	5.27E-03(1.00)	4.05E-02(1.00)	4.16E-01(1.00)	6.41E-03(1.00)	1.08E-04(2.00)	8.63E-06(2.12)
512	2.63E-03(1.00)	2.03E-02(1.00)	2.08E-01(1.00)	3.21E-03(1.00)	2.69E-05(2.00)	1.77E-06(2.29)

Table 4: Convergence of the H(div) finite element method for the manufactured test problem, with convergence rates in parentheses.

Notes

- Piecewise smooth manufactured test case [Tveito et al, 2017] ($\hat{J} = s$).
- Convergence rates as expected
- Second-order convergence in inf-norm interpolation/superconvergence artifact.
- Continuous and discrete Brezzi conditions hold under suitable compatibility assumptions on the finite element spaces and regularity of the domains. Literature?

A mortar finite element formulation of the EMI equations (I)

Assume K biological cells Ω_i^k with meshes $\mathcal{T}_{i,h}^k$, extracellular domain Ω_e with mesh $\mathcal{T}_{e,h}$, and membrane Γ_h:

$$\Gamma_h = \bigcup_{k=1}^{K} \Gamma_k \cup \bigcup_{g} \Gamma_g$$

Define finite element spaces:

$$U_e = \{v \in C^0(\mathcal{T}_{e,h}) \,|\, v|_T = \mathcal{P}_1(T) \,\forall\, T \in \mathcal{T}_{e,h}\},$$

$$U_i^k = \text{ same over } \mathcal{T}_{i,h}^k \text{ for each } k,$$

$$V = \{v \in C^0(\Gamma_h) \,|\, v|_\gamma = \mathcal{P}_1(\gamma) \,\forall\, \gamma \in \Gamma_h\}$$

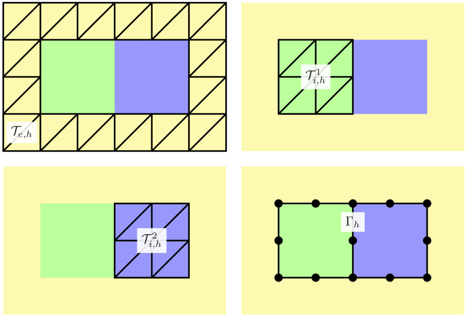

[Belgacem 1999; Lamichhane and Wohlmuth, 2004]

A mortar finite element formulation of the EMI equations (II)

Denote $J^i = J|_{\Gamma_i}$ for $\Gamma_i \subset \Gamma_h$ and $[\![u]\!]_{\Gamma_i}$ the jump in u across a membrane segment Γ_i.

Mortar finite element formulation

At each time step (or operator splitting step) with step size Δt, given $v \in V$, find the extracellular potential $u_e \in U_{e,h}$ and intracellular potentials $u_i^k \in U_{i,h}^k$ and membrane current densities $J \in V$ such that

$$
\begin{aligned}
(\sigma_i \operatorname{grad} u_i^k, \operatorname{grad} \phi_i^k) + (J^k, \phi_i^k)_{\Gamma_k} \pm (J^{g(k)}, \phi_i^k)_{\Gamma_{g(k)}} &= 0 && \forall\, \phi_i^k \in U_i^k, \forall\, k \\
(\sigma_e \operatorname{grad} u_e, \operatorname{grad} \phi_e) - \textstyle\sum_{k=1}^K (J^k, \phi_e)_{\Gamma_k} &= 0 && \forall\, \phi_e \in U_e \\
([\![u]\!]_{\Gamma_i}, \psi^i)_{\Gamma_i} - C_m^{-1}(\Delta t)(J^i, \psi^i)_{\Gamma_i} &= (v|_{\Gamma_i}, \psi^i)_{\Gamma_i} && \forall\, \psi \in V,\ \forall\, \Gamma_i \subset \Gamma_h
\end{aligned}
$$

Update $[\![u]\!]_{\Gamma_i} \mapsto v$ for each Γ_i.

[Agudelo-Toro and Neef, 2013; Tveito, Jæger, Kuchta, Mardal, R., 2017]

Mortar formulation converges at optimal rates for the EMI equations

n	$\|u - u_h\|_1$	$\|u - u_h\|_0$	$\|J - J_h\|_0$	$\|u - u_h\|_\infty$	$\|v - v_h\|_\infty$
16	1.11E+00(--)	2.85E-02(--)	1.45E-01(--)	6.36E-02(--)	5.03E-02(--)
32	5.59E-01(0.98)	7.37E-03(1.95)	4.01E-02(1.86)	2.09E-02(1.60)	1.82E-02(1.47)
64	2.80E-01(1.00)	1.90E-03(1.96)	1.05E-02(1.94)	6.73E-03(1.64)	6.22E-03(1.54)
128	1.40E-01(1.00)	4.99E-04(1.93)	2.65E-03(1.98)	2.15E-03(1.65)	2.08E-03(1.58)
256	7.02E-02(1.00)	1.38E-04(1.86)	6.66E-04(1.99)	6.93E-04(1.63)	6.90E-04(1.59)
512	3.51E-02(1.00)	4.16E-05(1.73)	1.66E-04(2.00)	2.31E-04(1.59)	2.34E-04(1.56)

Table 3: Convergence of the mortar finite element method for the manufactured test problem with convergence rates in parentheses.

Notes

- Piecewise smooth manufactured test case ([Tveito et al, 2017]).
- Convergence rates mostly as expected (superconv. in J artifact of test case?)
- Rates between $1 - 2$ closer to 2 for refined time discretization

The EMI framework allows for investigating fundamentally local variations in cell and membrane properties

Q: How do the spatial distribution of Na^+ channels affect the conduction velocity?

$$I_{\mathrm{ion}}(v) = I_{\mathrm{ion}}(v, s, g_{\mathrm{Na}}), \quad s_t = F(v, s, g_{\mathrm{Na}})$$

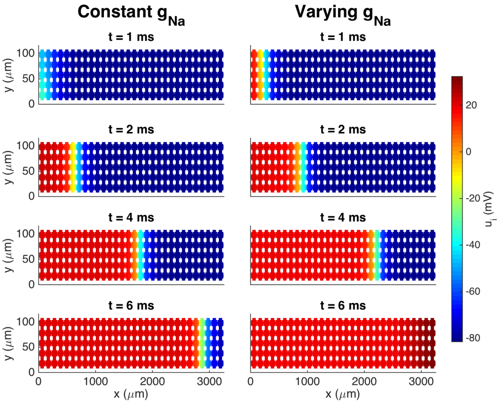

CV = 56.0 cm/s   CV = 65.5 cm/s

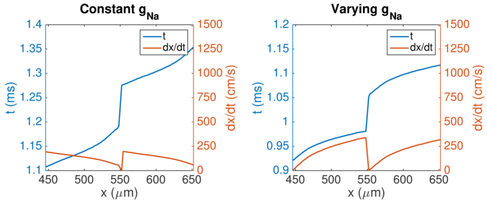

Activation times $t_{\min}|v(t) \geq 0$ (blue) and conduction velocities (orange) along length of two (biological) cells

A: Conduction velocity is increased for the case with a varying value of g_{Na} compared to the case with a constant value.

Collaborators

Matteo Croci (University of Oxford/Simula)
Per-Kristian Eide (Oslo University Hospital)
Patrick E. Farrell (University of Oxford)
Mike Giles (University of Oxford)
Janis Grobovs (University of Oslo)
Karoline Horgmo Jæger (Simula)
Miroslav Kuchta (University of Oslo)
Jeonghun Lee (ICES/UT Austin)
Kent-Andre Mardal (University of Oslo)
Eleonora Piersanti (Simula)
Aslak Tveito (Simula)
Vegard Vinje (Simula)

Core message

Mathematical models can give new insight into medicine, – and the human body gives an extraordinary rich setting for mathematics and numerics!

Thank you!

simula
waterscales
erc European Research Council Established by the European Commission
The Research Council of Norway